13

Development of an approach to parameterization of the SCC DFTB method for transition metals using copper oxide as an example

© P.A. Kolesnichenko,[1] O.E. Glukhova[1,2]

[1]Saratov National Research State University,
410012 Saratov, Russia
[2]I.M. Sechenov First Moscow State Medical University,
119991 Moscow, Russia
e-mail: glukhovaoe@info.sgu.ru

Received December 26, 2024
Revised December 26, 2024
Accepted December 26, 2024

A physico-mathematical toolkit for parameterizing the self-consisted charge density functional tight binding (SCC DFTB) has been developed by improving the algorithm for creating a new set of Slater-Koster basis functions. The purpose of the toolkit development is to increase the accuracy of theoretical prediction of the physical properties of nanostructures. The effectiveness of the improved parameterization algorithm of SCC DFTB method is demonstrated by the example of copper oxide (CuO). The obtained set of Slater-Koster basic functions demonstrates clear advantages over the well-known matsci-0-3 set: more accurate reproduction of the metric parameters of the crystal lattice (lengths of interatomic bonds and translation vectors) based on comparison with reliable experimental data; correspondence between the calculated and experimentally established band gap; correspondence of the calculated electrical conductivity of the crystal to experimental data.

Keywords: copper oxide, Slater-Koster parameters, quantum transport, SCC DFTB.

DOI: 10.61011/TP.2025.05.61139.466-24

Introduction

Today, one of the urgent problems of electronics and materials science is the development of sensor devices capable of ensuring safety of human life and contributing to improved quality of life in the environment. In this view, the area of improving the detection elements, i.e. air and gas sensors, is rapidly growing. Thin films of — quasi-2*D*-structures of metal oxides act as a sensitive element [1–3]. The high ratio between surface area and volume makes such structures ideal candidates as the basis for development of sensor devices for various purposes, including gas sensors, humidity sensors, photodetectors and biosensors [2].

Among the large number of varieties of metal oxides, copper oxide (CuO) stands out, which belongs to the semiconductors group with *p*-type conductivity [4]. Copper oxide-based materials are non-toxic and relatively inexpensive, so they are very cost-effective. These materials are widely used in photovoltaics, creation of lithium-ion batteries and electrochromic devices, supercapacitors and auto-emission cathodes [5,6].

For the effective use of any material, it is necessary to conduct predictive modeling, revealing its best properties and, as a result, the vector of development of its use [7–9]. The physical properties of 2*D*-/3*D*-copper oxide were analyzed *ab initio* and using semi-empirical methods, in particular, density functional test (DFT) and self-consisted charge density functional tight binding (SCC DFTB). At the same time, physically correct results are obtained with the correct calculation of the band structure, which determines the electronic, conductive and optical properties. For CuO crystals there's a problem of correct calculation of band structure and, hence, determination of the band gap (slit E_{gap}). From experimental data we know that $E_{gap} = 1.51$ eV [10–14], however, even DFT method in various software doesn't provide this slit width and gives it only within (1.40−1.48 eV) [15,16]. At the same time, DFT method requires large amounts of computational resources when calculating an electronic structure whose atomistic cell contains thousands or more atoms. An alternative option to DFT is SCC DFTB method which provides a possibility of studying materials with crystalline supercells containing several thousands atoms including atoms with *s*-, *p*-, *d*- and *f*-electrons [17–19]. However, the quality of the calculation results in this method is directly determined by the so-called „parameterization", determined by presence of an effective set of Slater-Koster basic functions (Slater-Koster-files or skf-files), which includes two parts: the first part, called „electronic part", contains integral tables — elements of Hamiltonian and overlap matrix; the second part, called „repulsive part", consists of the repulsion potentials of pairs of atomic nuclei and is written as splines. The presence of two parameterization parts makes it possible to calculate both the energy characteristics of the structure and to carry out molecular dynamics and search for the equilibrium configuration of the atomistic structure of crystalline supercells. To date several parameters sets are known: matsci-0-3 [20], pbc-0-3 [21], mio-0-1 [22], 3ob-3-1 [23] and others that are available at dftb.org [24].

These sets describe the interaction of atoms of chemical elements from 1st to 20-d number of periodic table and elements Ti, Fe, Ag, Au, As, Ga, Sc, Co, Ni, Zn and Eu. The disadvantage of these sets is the inability to correctly calculate the band structure of some pairs of atoms. In particular, for copper oxide, the set matski-0-3 significantly overestimates the slit (~ 3 eV) relative to the Egap values obtained by DFT method and the experimentally obtained value. In addition, the specified set incorrectly calculates the conductive properties of the crystal relative to experimental measurements. The purpose of this work is to expand the capabilities of SCC DFTB method by developing a new set of Slater-Koster parameters (sk-files — SK-files), including electronic and repulsive parts, for the correct calculation of electronic structure and studying the conductive properties of copper oxide crystal.

1. Mathematical modeling: approaches and methods

1.1. Fundamentals of SCC-DFTB method parameterization

The parameterization of the method is based on achieving a satisfactory consistency studied within SCC DFTB characteristics (in this case, the characteristics of zone structure and its profile) with the reference ones obtained using DFT method, correlating with the experimental ones within the error $\pm 5\,\%$.

SCC DFTB method — a semi-empirical quantum method based on a strong coupling approximation using a linear combination of atomic orbitals [25,26]. Expression for full energy E_{tot} also includes energy of zone structure E_{band}, SCC correction to Hamiltonian E_{scc} and repulsion potential E_{rep}. Full energy is described by the following equation (1):

$$E_{tot} = E_{band} + E_{scc} + E_{rep}. \tag{1}$$

Energy of zone structure E_{band} is calculated by summation of eigen values of ε Hamiltonian corresponding to the filled electron levels. The elements of Hamiltonian matrix are recorded as follows:

$$H^0_{\mu\nu} = \langle \psi_\mu \left| -\frac{1}{2}\nabla^2 + V_{\text{eff}}[\rho^0] \right| \psi_\nu \rangle, \tag{2}$$

where ψ_μ, ψ_ν wave functions, V_{eff} — effective potential defined by the energy of interaction of μ and ν orbitals which belong to two atoms a and b. Electron density ρ^0 is given by a sum of electron density on atom a and correction defined by the atom b: $\rho^0_a + \delta_{ab}\rho^0_b$. Single-center integrals are written as: $H^0_{\mu\nu} = \delta_{\mu\nu}\varepsilon_\mu$ (provided the equality of orbitals $\mu = \nu$) [27] is ensured, where ε_μ — are the eigen values of corresponding matrix elements in an isolated atom, and $\delta_{\mu\nu} = S_{\mu\nu}$ — overlap matrix. These integrals are calculated on a single atomic orbital and describe interactions that occur on a single atom, which is why they are called single-center. The double-center integrals $H^0_{\mu\nu}$ and $S_{\mu\nu}$ are calculated beforehand and listed in SK-files tables that are used further in SCC DFTB method. These integrals are the functions of distance and spatial atoms arrangement and are calculated by means of Slater-Koster transformation [28,29]. Non-diagonal elements of the Hamiltonian are described by the equation (2), and diagonal ones — by equation (3) [30]:

$$\left[-\frac{1}{2}\nabla^2 + V_{\text{eff}}[\rho^0] + V_{conf}\right]\psi_\nu(r) = \varepsilon_\nu \psi_\nu(r), \tag{3}$$

where r — distance, V_{conf} —- a polynomial limiting potential defined by the expression (4):

$$V_{conf} = \left(\frac{r}{r_0}\right)^s, \tag{4}$$

where r_0 and s — empirical parameters that may be selected randomly for each of the different orbital angular momentums and electron densityρ^0. This potential ensures retention of the electron density in a spherical region of radius r near the atom. As a rule, the parameter r_0 has a value approximately twice as large as the covalent radius of the atom [31]. With higher degree of polynomial s (called the degree or power of limitation), the electron density compression occurs more drastically and at short distances. It is the selection of parameters r_0 and s (for each angular momentum of atom, up to f-orbital) that allows providing identical band structures using SCC DFTB and DFT methods. The program „SKprogs“ [32] used in this paper allows varying the parameters r_0 and s for each atom orbital.

The second term of equation (1) —is the energy introduced to account for the change in electron density resulting from the interaction of atoms in the system. E_{scc} is expressed by the formula (5):

$$E_{scc} = \frac{1}{2}\sum_{\alpha,\beta}^{N} \Delta q_a \Delta q_b \gamma_{ab}, \tag{5}$$

where $\Delta q_a = \int \delta\rho^0_\alpha(r)dr^3$ — is fluctuation δ of the charge density ρ^0_α of atom a, which is calculated by Mulliken method [33]; γ_{ab} — is a parameter which stands for the Coulomb interaction of atom pairs. This parameter also includes the exchange-correlation interaction and Hubbard parameters. They are calculated for any atom within the local density approximation for the density functional theory (LDA-DFT) [34] or within the generalized gradient approximation (GGA-DFT) [35] used in this study.

The last term of equation (1) E_{rep} describes the repulsion between the nuclei that wasn't taken into account E_{band} and E_{scc}. This interaction is represented as the sum of the paired potentials between i, j atoms according to the formula (6):

$$E_{rep} = \sum_{i<j} V_{rep_{i,j}(r_{i,j})}, \tag{6}$$

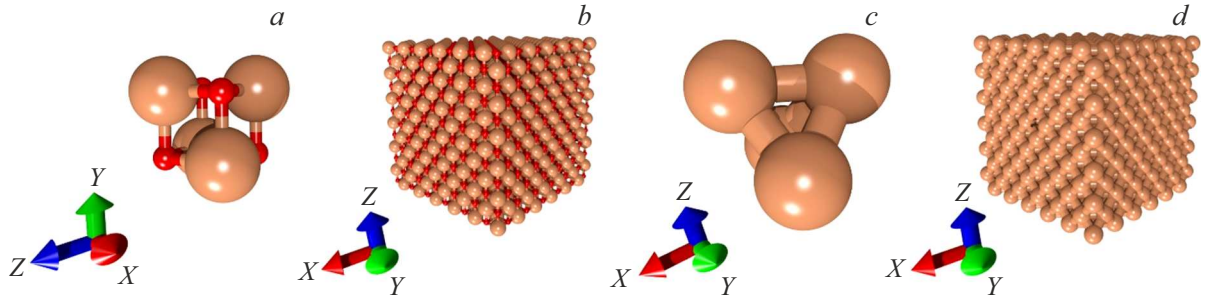

Figure 1. Model of copper oxide CuO (*a,b*) and metallic copper Cu (*c,d*). Lattice cell (*a* — CuO, *c* — Cu) and crystal element (*b* — CuO, *d* — Cu). Red color indicates oxygen, brown — copper.

where $V_{rep_{i,j}}$ — repulsive potential. Its search is a linear regression problem using polynomial functions. An example of a repulsive potential is the expression (7):

$$V_{rep}(r) = \sum_{p=2}^{6} c_p (r_{cut} - r)^p, \tag{7}$$

where r_{cut} — is the cutting radius, it is selected between the distances to the first and second nearest neighbor of the considered pair of atoms; c_p — weight coefficient. As a rule, the potential V_{rep} should be short-acting and decreasing as the distance between atoms increases. In this paper the repulsion potential was searched and built using „Tango“ program [36], where the cutting radii and the lowest and highest polynomial degrees varied.

1.2. Atomistic models of crystalline cells

CuO structures with the cubic lattice and symmetry group $F\overline{m}3m$ were selected for the study; here, the lattice cell consists of the four atoms of copper and four atoms of oxygen, and metallic copper Cu with cubic lattice and identical symmetry group where the lattice cell consists of four atoms of copper since they are widely used in the industry and chemistry as the nanostructures components [37–39] Lattice constant of CuO is equal 4.233 Å, that for Cu — 3.577 Å, which is consistent with experimental data [40,41]. These structures are shown in Fig. 1. The colored arrows show the directions of the axes in the Cartesian coordinate system.

1.3. General scheme of obtaining Slater-Koster parameters

To get the electronic configurations of the studied atoms „SKprogs“, software was used to find the repulsion potentials — „Tango“. Figure 2 shows a general flowchart for obtaining two parts of a set of parameters. The mechanism for creating parameters here is valid for any pairs of atoms of the periodic table elements. The flowchart is based on existing techniques for creating electronic [32] and repulsive [36] parts. The feature proposed in this paper is the principle of results verification and the error analysis of the method.

1.4. Getting electronic part of the set of parameters

First, the input data are entered into the program„SKprogs“. These are: type, mass, configuration of atom electronic shell (or pair of atoms). The second step includes entering the parameters for calculating overlap integrals, Hubbard parameters, and single-center integrals. Here the value r_0 (see equation(4)) for wave functions is given as the doubled covalent radius of the atom (initial value), and for density as tripled covalent radius. The limitation degree parameter s is 2, because using this value of this magnitude shows the correct results (e.g., in set pbc-0-3).

In the third step, the double-center integrals necessary to obtain the electronic configuration of a set of atoms are calculated. Using the earlier obtained electronic configurations the band structure of the studied objects was found by SCC DFTB methods and DFT method realized in code GPAW [42].

The fifth step includes comparison of band structures obtained by SCC DFTB and DFT methods. If the result is unsatisfactory, then using COBYLA method (Constrained Optimization BY Linear Approximation) a sequential selection of various input parameters takes place. The target function here is the minimum difference between the energy value of each point of the band at a certain point of reciprocal space for DFT and SCC DFTB methods.

For the structures studied in this paper, the fifth step has been changed. To obtain a set of parameters: before starting the parameters optimization using COBYLA method, in our case, the value r_0 was sorted for each atomic orbital. After finding the minima region in the energy band diagram DFT and SCC DFTB the improvement of parameters by COBYLA method was initiated for a more accurate finding of optimal value r_0. Next, if the difference between SCC DFTB and DFT was less than 5%, then, transition to the next global step was made — getting the repulsive

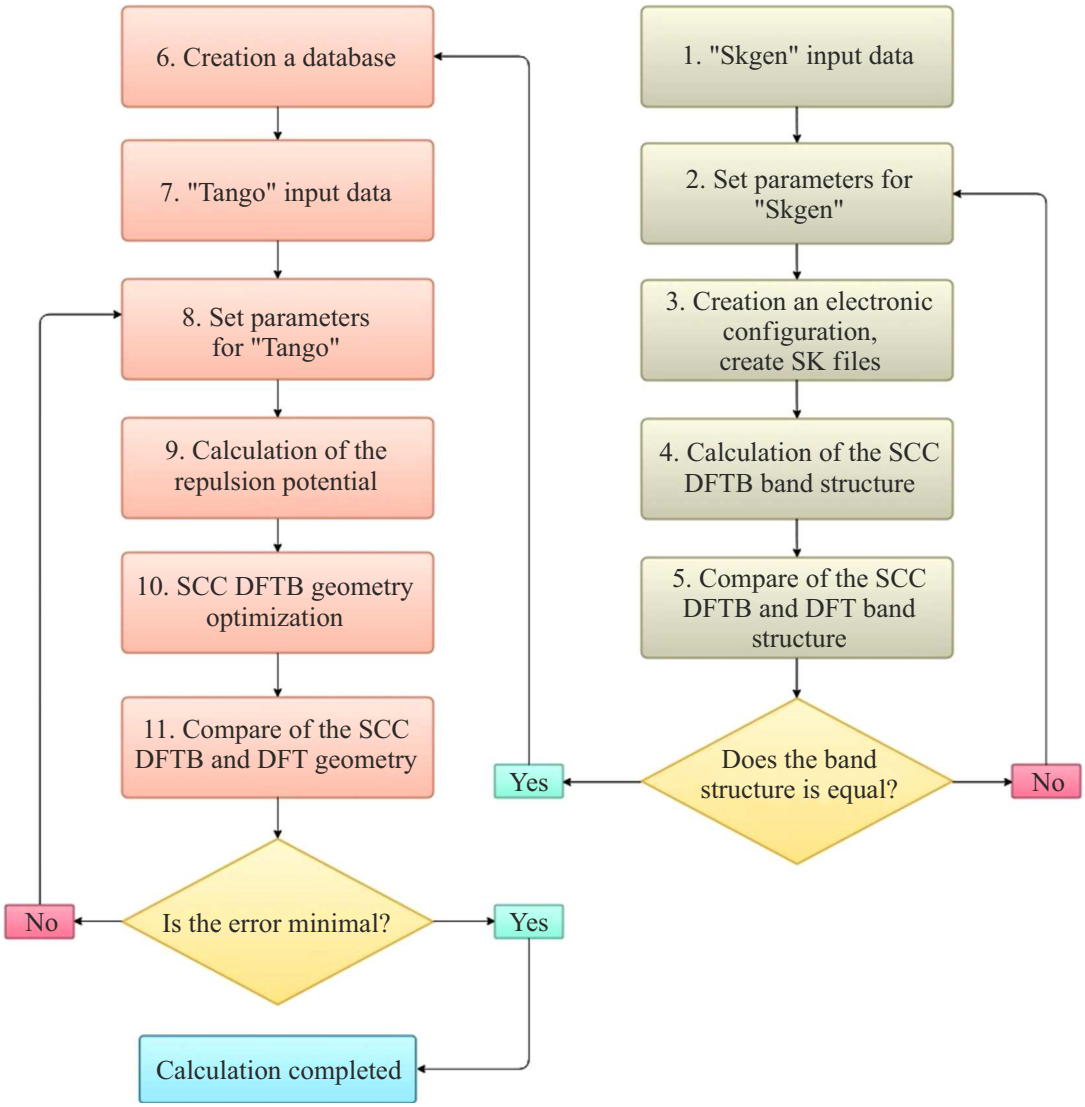

Figure 2. Flowchart for getting the set of parameters.

potential (step 6). If the difference is unsatisfactory then return is made to step 2.

Figure 3 shows the band structures of Cu and CuO crystals obtained using matski-0-3 parameters and parameters from this work in comparison with DFT calculation in GPAW program. The Brillouin zone bypass points correspond to a 3D crystal of copper and copper oxide. Yellow color shows DFT method, black — SCC-DFTB with appropriate parameters. The Fermi energy is assumed to be zero and is marked with a dotted line.

1.5. Getting electronic part of the set of parameters

After obtaining the electronic part of parameters, using *skf files from the fifth step, one may proceed to obtaining the repulsive part and calculating the repulsive potentials.

The sixth step consists in recording the geometric and energy parameters one by one after single-point DFT optimization with a step-by-step change in the initial atomistic structure (compression, stretching, twisting and separation of the atom) of the studied supercells. In this paper the supercells were scaled in isotropic way within the range from 99 % to 131 % of initial volume with an increment of 1 %.

Introductory data for „Tango“ program: type, configuration of the electronic shell, maximum angular momentum, database used.

The eighth step sets the values for the minimum ($r_{\min}$) and maximum (r_{cut}) distance between atoms, at which the repulsive potential is determined. Also the degree of polynomial is specified (see. equation (7)).

In the ninth step, the repulsive potential is calculated in „Tango“ program. The results are recorded in previously received SK-files containing the electronic configuration.

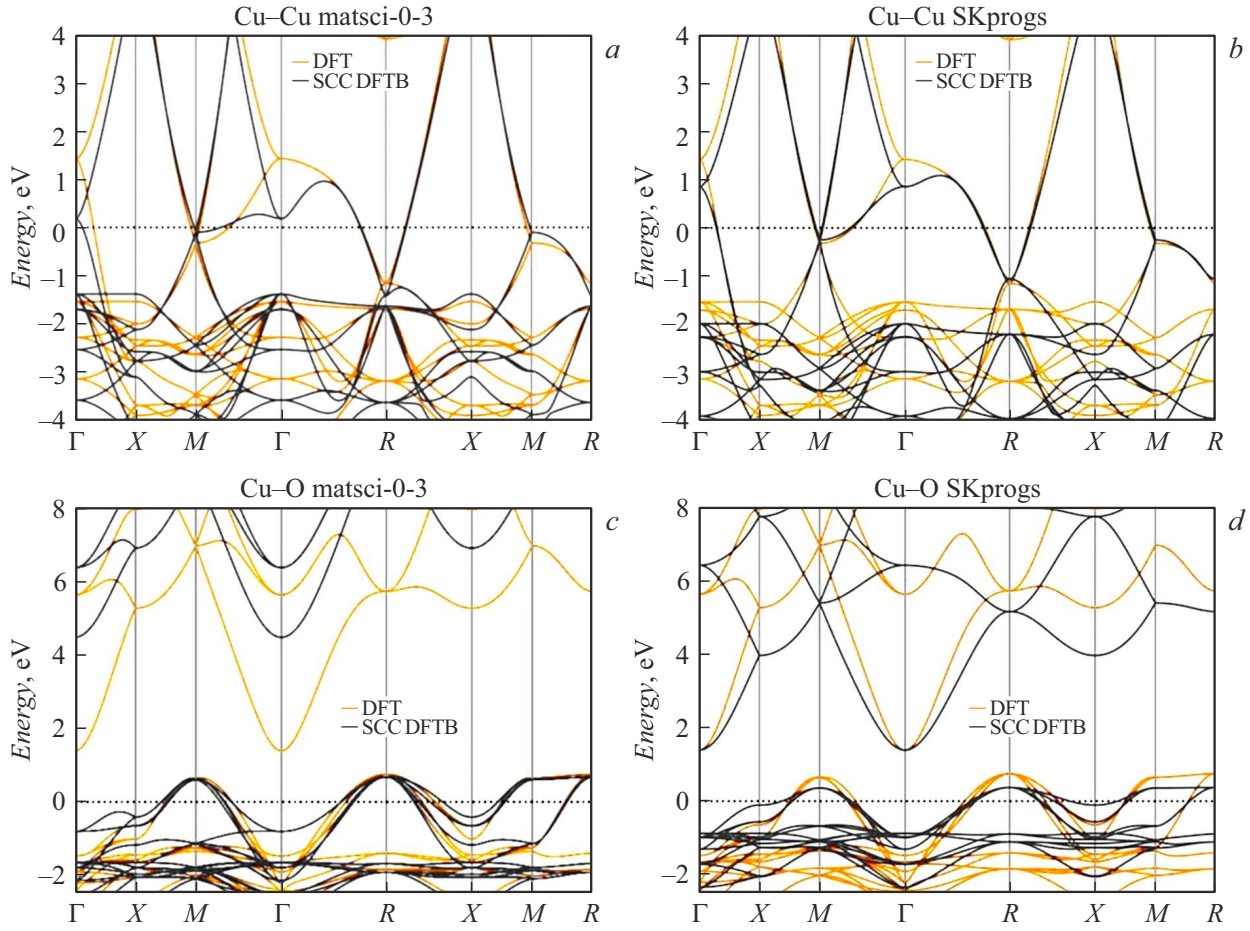

Figure 3. Band structures of metallic copper (Cu-Cu), obtained using parametersmatsci-0-3 (*a*) and parameters outlined in this paper (*b*). The same is for (Cu-O) copper oxide with parameters matsci-0-3 (*c*) and parameters from this paper (*d*).

The tenth step involves varying the coordinates and lengths of the translation vectors in the structure to find the minimum total energy using the repulsive potentials of the studied pairs of atoms obtained in the previous step using SCC DFTB method.

At the last step, the atomistic structure obtained in the previous step is compared with the reference structure obtained by DFT method. The lengths of the translation vectors of the structures and the lengths of the interatomic bonds are compared. The error is calculated as a percentage for each value, after which the total error for this structure is calculated. If the error is less than 5 %, then, the calculation is finished. Otherwise — return to step 8 with other parameters.

The repulsive potentials obtained in this work for the studied pairs of atoms in comparison with similar splines from the set matsci-0-3 are shown in Fig. 4.

As a result, a new set of Slater-Koster parameters for Cu and CuO crystals was obtained, which ensures that the band gap coincides with the experiment and that the results of optimizing the atomistic structure are close to the results of DFT. The calculation error is no more than 1.5 %

2. Results

2.1. Improvement of atomistic structure

The obtained repulsive potentials were verified by optimizing the studied atomistic structures. The optimization process consisted in searching for geometric parameters (translation vector lengths, atomic coordinates) at which a global minimum of energy was observed. A comparison of the optimization results using parameters from this work with parameters matsci-0-3 and the results of DFT optimization (taken as a reference) is shown in the table.

A zero error corresponds to a complete match of the compared value with the reference value. The error was calculated by formula (8):

$$L_{error} = \left| \left(\frac{L_{DFT} - L_{params}}{L_{DFT} + L_{params}} \right) \Big/ 2 \right| \cdot 100\,\%. \qquad (8)$$

The average error value was calculated as the arithmetic mean of the sum of all error values L_{error}.

As can be seen, the error when using the parameters from this work decreased by nine times compared to the set matsci-0-3 for metallic copper (Cu-Cu), and by one and

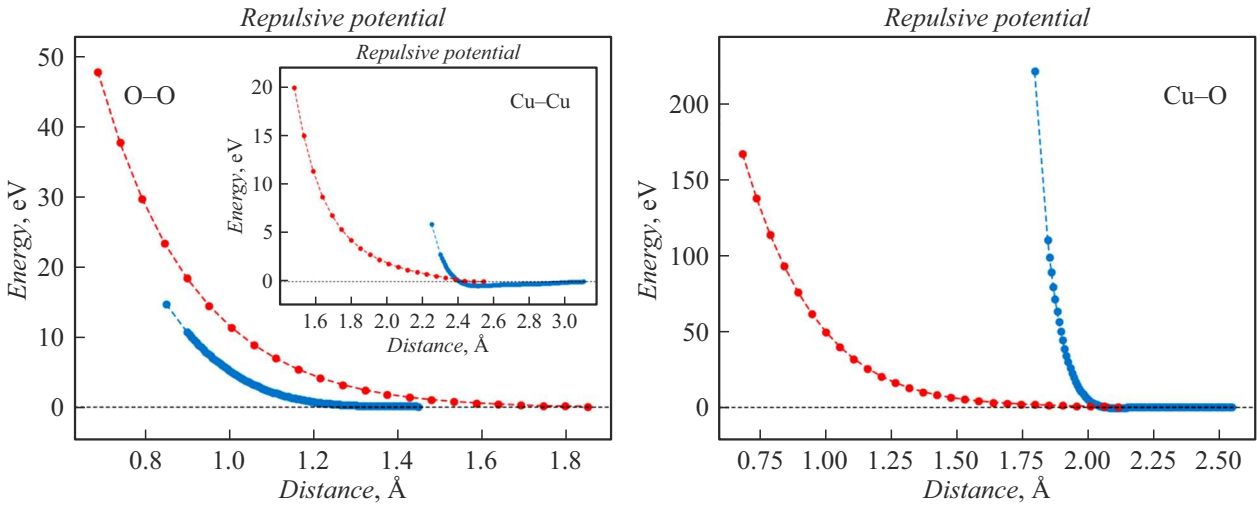

Figure 4. Graph of repulsive potential of the pairs of atoms Red color shows the potential from the set matsci-0-3, blue — obtained in this paper.

Comparison of the results of atomistic structure optimization

Compared value	Cu-Cu		O-O		Cu-O	
	matsci-0-3 error, %	This study error, %	matsci-0-3 error, %	This study error, %	matsci-0-3 error, %	This study error, %
Translation vector length along X axis	4.54	0.02	–	–	2.78	0.004
Translation vector length along Y axis	4.54	0.02	–	–	2.78	0.004
Translation vector length along Z-axis	4.54	0.02	–	–	2.78	0.004
Bond length	0.77	0.01	1.49	1.07	0.67	0.07
Average error	3.60	0.40	1.49	1.07	2.23	1.26

a half times for copper oxide (Cu-O). Fig. 5 illustrates the models of the studied structures, where optimization of geometry was performed by DFT method, as well as by SCC DFTB method with parametersmatsci-0-3 and parameters of this study.

When using parameters obtained in this work, the positions of atoms do not visually change relative to DFT optimization. For the set matsci-0-3 there's an error in atoms position which is highlighted by red in Fig. 5, *c*.

2.2. Conductivity calculation

The obtained parameters were used to calculate the electrical conductivity of copper oxide using the theory of quantum electron transport. The graph of T-transmission function depending on energy is given in Fig. 6. The resistance was calculated using the theory of quantum electron transport using Landauer-Buttiker formalism and Green-Keldysh function apparatus [43]. It allows calculating the electrical conductivity based on the electron transmission function T(E):

$$G = \frac{2e^2}{h} \int_{-\infty}^{\infty} T(E) F_T(E - E_F) dE, \qquad (9)$$

where e — electron charge; h — Planck constant; e^2/h — conductivity quantum, value for the single conductivity channel. This value doubles to account for the electrons spin; $F_T(E)$ — the so-called function of thermal broadening calculated by formula (10):

$$F_T(E) = \frac{1}{4k_B T} sech\left(\frac{E}{2k_B T}\right), \qquad (10)$$

where k_B — Boltzmann constant; T — temperature. From the above formulae it was calculated that the conductivity G of CuO crystal is equal $3.7 \cdot 10^{-4}$ S·cm. Resistance R accordingly was $2.7 \cdot 10^3$ Ω·cm. This value is consistent

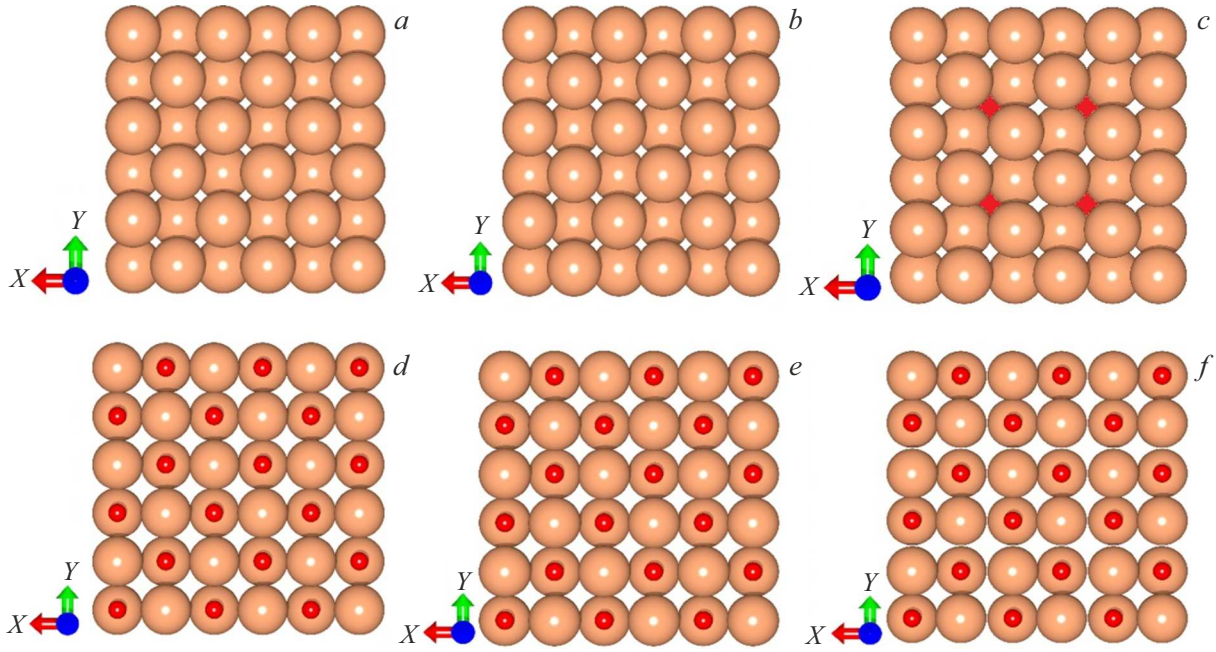

Figure 5. Results of the atomistic structure optimization. Reference supercell of copper (*a*) and copper oxide (*d*); copper (*b*) and copper oxide (*e*) supercell improved with parameters from this study; supercell of copper (*c*) and copper oxide (*f*) improved with parametersmatsci-0-3

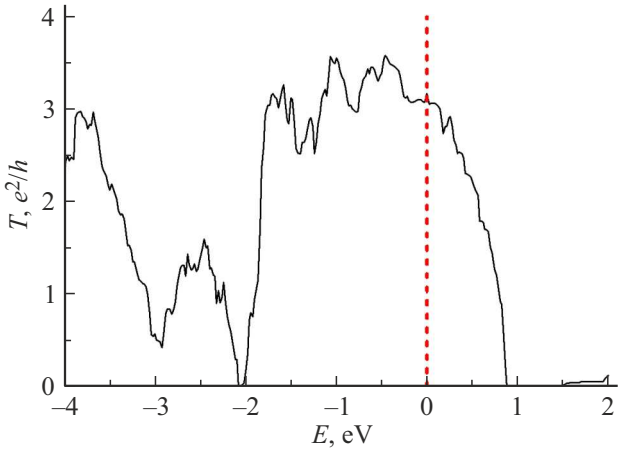

Figure 6. Graph of transmission function for CuO. Red line shows Fermi level.

with the experimental value, which lies within the range of $10^2 - 10^4\,\Omega\cdot$cm [44,45]. This confirms the correctness of the obtained parameters and their applicability in solving practical problems.

Conclusion

A new parameterization in the form of Slater-Koster sets for copper oxide and metallic copper crystals has been developed. It is shown that the band structure with this parameterization, calculated using ISCC DFTB method, repeats the band structure calculated by DFT method, while the width of CuO band gap also coincides. Similarly, the results of optimization of the atomistic structure of the studied crystals coincide with an accuracy of 1%. The resistance of the crystal was measured using Landauer-Buttiker theory of quantum transport, the result in 2.7 kΩ is consistent with experimental data. This opens up great opportunities in the field of predictive modeling. In particular, thanks to the results of the work, it becomes possible to study copper oxide as a detecting element of gas sensors. For such studies, a large cell is required so that when the assays are planted on the surface, they do not interact with each other. An additional complication is that the study requires a surface, which needs that a certain number of thin layers of the structure have electronic properties of a three-dimensional crystal. A similar technique has previously been tested for zinc oxide crystals (ZnO) [46]. Due to these conditions, the number of atoms in a cell can be large, which will require significant computing resources. All these difficulties can be overcome successfully using the new parameterization of SCC DFTB method.

Conflict of interest

The authors declare that they have no conflict of interest.

References

[1] S. Steinhauer. Chemosensors, **9**, 51 (2021). DOI: 10.3390/chemosensors923–271

[2] D. Nunes, A. Pimentel, A. Gonçalves, S. Pereira, R. Branquinho, P. Barquinha, E. Fortunato, R. Martins. Semicond. Sci. Technol., **34**, 043001 (2019). DOI: 10.1088/1361-6641/ab011e
[3] P.T. Moseley. Meas. Sci. Technol., **28**, 082001 (2017). DOI:10.1088/1361-6501/aa7443
[4] H.J. Kim, J.H. Lee, Sens. Actuators B Chem., **192**, 607 (2014). DOI: 10.1016/j.snb.2013.11.005
[5] A.S. Zoolfakar, R.A. Rani, A.J. Morfa, A.P. O'Mullane, K. Kalantar-zadeh. J. Mater. Chem. C, **2**, 5247 (2014). DOI: 10.1039/C4TC00345D
[6] Q. Zhang, K. Zhang, D. Xu, G. Yang, H. Huang, F. Nie, C. Liu, S. Yang. Prog. Mater. Sci., **60**, 208 (2014). DOI: 10.1016/j.pmatsci.2013.09.003
[7] S. Zhaoxiang, R.I. Sosa, S.P.A. Bordas, A. Tkatchenko, J. Lengiewicz. Intern. J. Eng. Sci., **204**, 104126 (2024). DOI: 10.1016/j.ijengsci.2024.104126
[8] M. Damej, A. Molhi, H. Lgaz, R. Hsissou, J. Aslam, M. Benmessaoud, N. Rezki, H-S. Lee, D-E. Lee. J. Molecular Structure, **1273** 134232 (2023). DOI: 10.1016/j.molstruc.2022.134232
[9] Y. Han, L. Wu, Z. Wang, S. Wang, Z. Qian. Mater. Today Commun., **34**, 105233 (2023). DOI: 10.1016/j.mtcomm.2022.105233
[10] T. Minami, Y. Nishi, T. Miyata, J.I. Nomoto. Appl. Phys. Express, **4**, (2011). DOI: 10.1143/APEX.4.062301
[11] N. Serin, T. Serin, S. Horzum, Y. Celik. Semicon. Sci. Technol., **20**, 398 (2005). DOI:10.1088/0268-1242/20/5/012
[12] P. Sawicka-Chudy, M. Sibiński, G. Wisz, E. Rybak-Wilusz, M. Cholewa. J. Phys.: Conf. Ser., **1033** 012002 (2018). DOI:10.1088/1742-6596/1033/1/012002
[13] J.-Y. Parka, C.-S. Kimb, K. Okuyamac, H.-M. Leed, H.-D. Jange, S.E. Leef, T.-O. Kima. J. Power Sources, **306**, 764 (2016). DOI: 10.1016/j.jpowsour.2015.12.087
[14] M. Ichimura, Y. Kato. Mater. Sci. Semicond. Process., **16** (6), 1538 (2013). DOI: 10.1016/j.mssp.2013.05.004
[15] N.J. Zainab, A.M. Hussein, M. Mahbubur Rahman, A. Amri, Zh.-T. Jiang. Canadian J. Phys., **102** (5), 316 (2024). ISSN 0008-4204, DOI: 10.1139/cjp-2023-0241
[16] M. Nolan, S. Elliott. Phys. Chem. Chem. Phys.: PCCP, **8**, 5350-8 (2006). DOI: 10.1039/b611969g
[17] H. Liu, G. Seifert, C. Di Valentin. J. Chem. Phys., **150** (9), 094703 (2019). DOI: 10.1063/1.5085190
[18] G. Zheng, S. Irle, K. Morokuma. Chem. Phys. Lett., **412** (1–3), 210 (2005). DOI: 10.1016/j.cplett.2005.06.105
[19] S. Manzhos. Chem. Phys. Lett., **643**, 16 (2016). DOI: 10.1016/j.cplett.2015.11.007
[20] N. Jardillier, Ph.D. Thesis. Universite Montpellier II, (2006). http://nicolas.jardillier.free.fr. (access date: 10.11.2024).
[21] E. Rauls, R. Gutierrez, J. Elsner, Th. Frauenheim. Sol. State Comm., **111**, 459 (1999). DOI: 10.1016/S0038-1098(99)00137-4
[22] M. Gaus, Q. Cui, M. Elstner. J. Chem. Theory Comput., **7**, 931 (2011). DOI: 10.1021/ct100684s
[23] M. Kubillus, T. Kubař, M. Gaus, J. Řezáč, M. Elstner. J. Chem. Theory Comput., **11**, 332 (2015). DOI: 10.1021/ct5009137
[24] Electronic resource. Available at: https://dftb.org/ (Date of access: 13.11.2024).
[25] P. Koskinen, V. Makinen. Comput. Mater. Sci., **47**, 237 (2009). DOI: 10.48550/arXiv.0910.5861
[26] M. Wahiduzzaman, A.F. Oliveira, P. Philipsen, L. Zhechkov, E. van Lenthe, H.A. Witek, T. Heine. J. Chem. Theory Comp., **9** (9), 4006 (2013). DOI:10.1021/ct4004959
[27] G. Kresse, D. Joubert. Phys. Rev., **59**, 1758 (1999). DOI: 10.1103/PhysRevB.59.1758
[28] T. Frauenheim, G. Seifert, M. Elstner, Z. Hajnal, G. Jungnickel, D. Porezag, S. Suhai, R.A. Scholz. Phys. Status Solidi B, 217, 41 (2000). DOI: 10.1002/(SICI)1521-3951(200001)217:1¡41::AID-PSSB41¿3.0.CO;2-V
[29] J.C. Slater, G.F. Koster. Phys. Rev., **94** (6), 1498 (1954). DOI:10.1103/physrev.94.1498
[30] Y. Di, Q. Zongyang, L. Pai, L. Zhenyu. Acta Phys. Chim. Sin., **34** (10), 1116 (2018). DOI: 10.3866/PKU.WHXB201801151
[31] B. Grundkötter-Stock, V. Bezugly, J. Kunstmann, G. Cuniberti, T. Frauenheim, T.A. Niehaus. J. Chem. Theory Comp., **8** (3), 1153 (2012). DOI:10.1021/ct200722n
[32] B. Aradi, T. van der Heide, B. Hourahine, Z. Hu, C. Kóhler, T. Niehaus. [Source code] https://github.com/dftbplus/skprogs. (access date: 09.11.2024)
[33] R.S. Mulliken. J. Chem. Phys., **23**, 1833 (1955). DOI:10.1063/1.1740588
[34] M. Lewin, E.H. Lieb, R. Seiringer. Pure Appl. Analysis, **2** (1), 35 (2020). DOI:10.2140/paa.2020.2.35
[35] J.P. Perdew, J.A. Chevary, S.H. Vosko, K.A. Jackson, M.R. Pederson, D.J. Singh, C. Fiolhais. Phys. Rev. B, **46**, 11 6671 (1992). DOI: 10.1103/physrevb.46.6671
[36] M. Van den Bossche, H. Grónbeck, B. Hammer. J. Chem. Theory Comp., **14** (5), 2797 (2018). DOI: 10.1021/acs.jctc.8b00039
[37] R.K. Cheedarala, J.I. Song. Intern. J. Heat and Mass Transfer, **162**, 120391 (2020). DOI: 10.1016/j.ijheatmasstransfer.2020.120391
[38] L. Guo, F. Tong, H. Liu, H. Yang, J. Li. Mater. Lett., **71**, 32 (2012). DOI: 10.1016/j.matlet.2011.11.105
[39] J. Singh, A.K. Manna, R.K. Soni. Appl. Surf. Sci., **530**, 147258 (2020). DOI: 10.1016/j.apsusc.2020. 147258
[40] T. Chen, T. Zhang, G. Wang, J. Zhou, J. Zhang, Yu. Liu. J. Mater. Sci., **47** (11), 4612 (2012). DOI: 10.1007/s10853-012-6326-1
[41] K. Lejaeghere, V. Van Speybroeck, G. Van Oost, S. Cottenier. Critical Rev. Solid State Mater. Sci., **39**, 1 (2014). DOI: 10.1080/10408436.2013.772503
[42] J.J. Mortensen, A.H. Larsen, M. Kuisma, A.V. Ivanov, A. Taghizadeh, A. Peterson, A. Haldar, A.O. Dohn, C. Schäfer, E.Ö. Jónsson, E.D. Hermes, F.A. Nilsson, G. Kastlunger, G. Levi, H. Jónsson, H. Häkkinen, J. Fojt, J. Kangsabanik, J. Sødequist, J. Lehtomäki, J. Heske, J. Enkovaara, K.T. Winther, M. Dulak, M.M. Melander, M. Ovesen, M. Louhivuori, M. Walter, M. Gjerding, O. Lopez-Acevedo, P. Erhart, R. Warmbier, R. Würdemann, S. Kaappa, S. Latini, T.M. Boland, T. Bligaard, T. Skovhus, T. Susi, T. Maxson, T. Rossi, X. Chen, Y.L.A. Schmerwitz, J. Schiøtz, T. Olsen, K.W. Jacobsen, K.S. Thygesen. J. Chem. Phys., **160**, 092503 (2024). DOI: 10.1063/5.0182685
[43] S. Datta. *Electronic Transport in Mesoscopic Systems* (Cambridge: Cambridge University Press, 1995), 396 p.
[44] A.A. Ogwu, T.H. Darma, E. Bouquerel. J. Achievements Mater. Manufacturing Eng., **4** (1), 172 (2007).

[45] L. De Los Santos Valladares, D.H. Salinas, A.B. Dominguez, D.A. Najarro, S.I. Khondaker, T. Mitrelias, C.H.W. Barnes, J.A. Aguiar, Y. Majima. Thin Solid Films, **520** (20), 6368 (2012). DOI: 10.1016/j.tsf.2012.06.043
[46] O.E. Glukhova, P.A. Kolesnichenko. Tech. Phys., **69** (2), 300 (2024). DOI: 10.21883/0000000000

Translated by T.Zorina